Theory of the Ablative Richtmyer–Meshkov Instability

In inertial confinement fusion (ICF) implosions, a laser irradiation induces a shock wave propagating through the target. During the shock transit time, the ablation front travels at a constant velocity, and any surface perturbations could grow due to the Richtmyer-Meshkov (RM)–like instability.[1–5] Later, when a rarefaction wave reaches the ablation surface, the acceleration of the interface becomes finite, and ablation-front perturbations (multiplied by the RM growth) grow due to the Rayleigh–Taylor (RT) instability. It is important to study the perturbation evolution during the shock transit time mainly for two reasons: (1) to determine the initial conditions for the RT phase of instability and (2) to analyze the level of laser imprint on directly driven ICF targets.

The RM instability occurs when a plane shock interacts with a corrugated interface between two fluids (see Fig. 77.30). As a result of such an interaction, interface perturbation starts to grow because the transmitted shock is converging at the peak (point A) and diverging at the valley (point B). Converging shock increases pressure and accelerates perturbation peak into fluid 2. Similar instability occurs at the distorted interface of an ablatively driven target, where ablation pressure generates a rippled shock that induces pressure perturbation at the ablation front and causes distortion growth. The classical treatment of the RM problem leads to a linear-in-time asymptotic perturbation growth[1] $\eta(kc_s t >> 1) \simeq \eta_0 kc_s t$, where η is the interface perturbation, k is the mode wave number, c_s is the sound speed of the compressed material, and η_0 is a constant depending on the initial conditions. Recent studies showed that the ablation of material from the target surface turns such a growth into damped oscillations.[4,5] During the last two years, several researchers have made attempts to develop an analytic theory of the ablative Richtmyer–Meshkov instability. In Refs. 4 and 5, the authors, on the basis of a gas dynamic model, found saturation of perturbations. At the ablation front, however, they used an heuristic boundary condition that, as will be shown later, contradicts the result of the self-consistent theory.[6–8] In Ref. 3 the boundary conditions at the ablation front were derived by using the Chapman–Jouget deflagration model. As criticized in Ref. 5, however, this model does not give an adequate description of the ablative process. In this article, we develop a sharp-boundary model to study the imposed mass-perturbation growth during the shock-transit time. The boundary conditions at the shock front are derived using the Hugoniot relations. At the ablation front the result of the self-consistent analysis[6–8] is applied, and it is shown that the asymptotic behavior of the ablation-front perturbations is quite different from the earlier theoretical predictions.[3–5] In particular, the dynamic overpressure causes

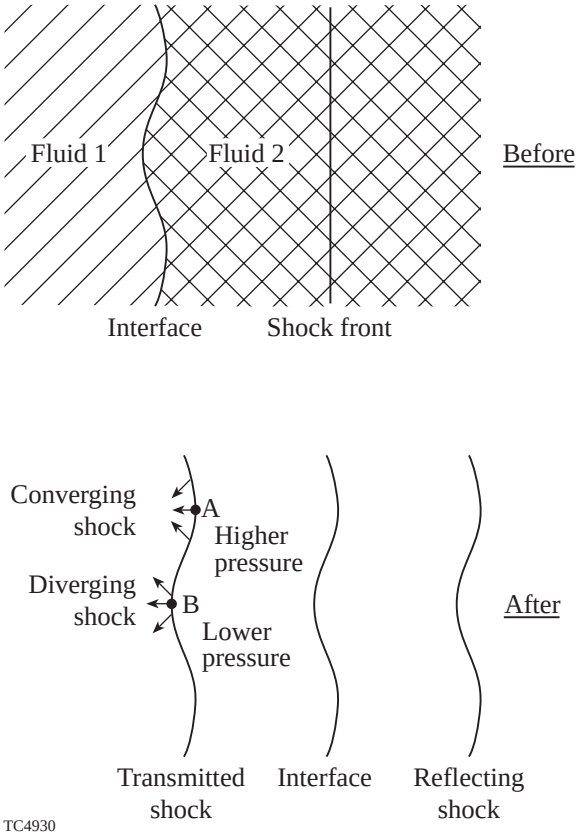

Figure 77.30
Richtmyer–Meshkov instability occurs when a plane shock interacts with a corrugated interface between two fluids.

perturbation oscillations in time (in agreement with the numerical results)[2,5] with the frequency $\omega = k\sqrt{V_a V_{\rm bl}}$ and the amplitude $\eta_0 c_s/\sqrt{V_a V_{\rm bl}}$, where V_a and $V_{\rm bl}$ are the ablation and blow-off velocity, respectively. In addition, the mass ablation damps the oscillation amplitude on a time scale $1/(kV_a) >> 1/\omega$.

To study the linear perturbation growth during the shock-transit time, we consider a sharp-boundary model and identify the following three constant-density regions (see Fig. 77.31): (1) uncompressed material (undriven portion of the target) $y < y_s$ ($\rho = \rho_1$), (2) material compressed by the shock $y_s < y < y_a$ ($\rho = \rho_2$), and (3) ablated plasma $y > y_a$ with the density $\rho = \rho_3$. In the ablation-front frame of reference, the compressed material and blowoff plasma are moving in a positive y direction with velocities V_a and $V_{\rm bl} = V_a\rho_2/\rho_3$, respectively. In the shock-front frame of reference, the undriven- and compressed-fluid velocities are $U_1 = \sqrt{\rho_2/\rho_1(P_2 - P_1)/(\rho_2 - \rho_1)}$ and $U_2 = \rho_1 U_1/\rho_2$, where $P_{1(2)}$ is the pressure in the region 1(2).

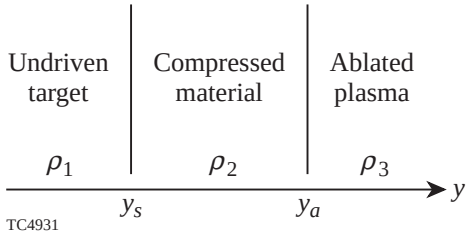

Figure 77.31
The equilibrium configuration is represented by the three regions (1) undriven target, (2) compressed material, and (3) ablated plasma.

The stability analysis of the described equilibrium is performed in the standard fashion. First, all perturbated quantities are decomposed in the Fourier space $Q_1 = \tilde{Q}(y,t)e^{ikx}$. Then, in the frame of reference moving with the compressed-region velocity, the linearized conservation equations are combined into a single partial differential equation for the pressure perturbation $\tilde{p}$:[1,3,9]

$$\partial_t^2 \tilde{p} - c_s^2 \partial_y^2 \tilde{p} + k^2 c_s^2 \tilde{p} = 0, \tag{1}$$

where c_s is the sound speed of the compressed material. The boundary conditions at the ablation front can be derived by integrating the perturbed conservation equations across the interface $y = y_a$. The result is

$$\frac{\tilde{v}_x - \tilde{v}_x^l}{c_s} = i\zeta_a\Omega(1-\delta),\ (1-\delta)\,d_\tau\zeta_a = \tilde{v}_y - \delta\,\tilde{v}_y^l,$$
$$\tilde{w} - \tilde{w}^l = 2\frac{V_a}{c_s}\Omega(1-\delta)\zeta_a, \tag{2}$$

where superscript l denotes the blowoff region variable, $\Omega = V_{\rm bl}/c_s$, $\delta = \rho_3/\rho_2$, $\tau = kc_s t$, $\tilde{w} = \tilde{p}/(\rho_2 c_s^2)$, and $\zeta_a = k\eta_a$ is the normalized ablation-surface perturbation. It is well known[10,11] that the sharp-boundary model cannot be solved in closed form in the presence of ablation without a supplementary boundary condition at the surface of discontinuity. The closure equation can be derived only by using the self-consistent stability analysis of ablation fronts. In Refs. 6–8 such an analysis was carried out by keeping finite thermal conductivity in the energy-conservation equation. Taking the limit of zero ablation-front thickness in the analytical solution, one can derive the jump conditions for the hydrodynamic quantities at the ablation front.[8,10] In addition to the conditions (2), the following jump in the perturbed transverse velocity is found:

$$\tilde{v}_y - \tilde{v}_y^l = -\zeta_a V_{\rm bl}(1-\delta). \tag{3}$$

Observe that by combining Eqs. (2) and (3) one can derive an equation for the perturbation evolution $d_t\eta_a + kV_a\eta_a = \tilde{v}_y$ that contradicts the boundary condition chosen heuristically in Eq. (10) of Ref. 5. At the shock front the boundary conditions are obtained by using the perturbed Hugoniot relations. The details of calculation can be found in Ref. 9. Next, to simplify the matching procedure we introduce new variables $r = \sqrt{\tau^2 - k^2y^2}$ and $\theta = \tanh^{-1}(ky/\tau)$; then Eq. (1) and the boundary conditions at the shock and ablation fronts take the following form:

$$\partial_r^2\tilde{w} + \frac{1}{r}\partial_r\tilde{w} + \tilde{w} - \frac{1}{r^2}\partial_\theta^2\tilde{w} = 0, \tag{4}$$

$$\tilde{w}_s = \frac{L_1}{\cosh\theta_s}d_r\zeta_s, \tag{5}$$

$$\partial_\theta\tilde{w}_s = -rL_3\frac{\sinh^2\theta_s}{\cosh\theta_s}\zeta_s - \frac{rL_2}{\cosh\theta_s}d_r^2\zeta_s, \tag{6}$$

$$(1-\delta)\,d_r^2\zeta_a - \delta\,\Omega^2\zeta_a + \frac{\partial_\theta \tilde{w}_a}{r} + \tilde{w}_a = O\left(\delta^2\right), \qquad (7)$$

$$d_r\left(\delta\,\Omega d_r\zeta_a + \delta\,\Omega^2\zeta_a - \tilde{w}_a\right) = \delta\,\Omega\tilde{w}_a + \delta^2\Omega^2 F(r) + O\left(\delta^3\right), \qquad (8)$$

where $\tanh\theta_a = -V_a/c_s$, $\tanh\theta_s = -U_2/c_s$, $\tilde{w}_s = \tilde{w}\left(r,\theta_s\right)$, $\tilde{w}_a = \tilde{w}\left(r,\theta_a\right)$, and

$$L_1 = \frac{4}{\gamma+1}\tanh\theta_s,\quad L_2 = 2\frac{M_1^2+1}{M_1^2(\gamma+1)},$$

$$L_3 = 2\frac{M_1^2-1}{2+(\gamma-1)M_1^2},$$

$$F(r) = \frac{1}{L_1}\left(\frac{4}{\gamma+1} - L_2 - L_3\right)\tilde{w}\left(\frac{-\delta\,\Omega r}{\sinh\theta_s},\theta_s\right).$$

Here $M_1 = U_1/c_1$ is the shock Mach number, and c_1 is the sound speed of the undriven material. A general solution of Eq. (4) can be written as an infinite sum of Bessel functions $J_\mu(r)$:[3,9]

$$\tilde{w} = \sum_\mu \left(M_\mu\cosh\mu\theta + N_\mu\sinh\mu\theta\right)\,J_\mu(r), \qquad (9)$$

where constants M_μ and N_μ are determined from the boundary conditions (5)–(8). The temporal evolution of the front-surface perturbations is described by Eqs. (7) and (8) that can be solved by using the multiple-scale analysis. Next, we introduce a long-scale variable $T = \sqrt{\delta}r$ and make the following ordering: $\Omega \sim 1$, $\left(V_a/c_s\right) \sim \delta << 1$. Also we assume that

$$\tilde{w}_a \sim \delta,\ \partial_r\tilde{w}_a \sim \delta,\ \partial_\theta\tilde{w}_a \sim 1. \qquad (10)$$

The last assumptions will be verified *a posteriori*. The system (7)–(8) then reduces to

$$\partial_r^2\zeta_a + 2\sqrt{\delta}\partial_{rT}^2\zeta_a + \delta\,\partial_T^2\zeta_a + \delta\ \Omega\partial_r\zeta_a + \delta^{3/2}\Omega\partial_T\zeta_a + \frac{\partial_\theta\tilde{w}_a}{r} = f(T), \qquad (11)$$

$$\partial_r^2\zeta_a + 2\sqrt{\delta}\partial_{rT}^2\zeta_a + \Omega\partial_r\zeta_a + \sqrt{\delta}\Omega\partial_T\zeta_a + \Omega^2\zeta_a - \frac{\tilde{w}_a}{\delta} = f(T), \qquad (12)$$

where $f(T)$ satisfies the first-order differential equation

$$d_T f(T) = \Omega\tilde{w}_a\big/\sqrt{\delta} + \sqrt{\delta}\,\Omega^2 F(T).$$

In Eqs. (11) and (12) the ablation-front perturbation ζ_a and constants N_μ and M_μ are expanded in powers of δ: $Q = Q^0 + \delta Q^1 + \ldots$. To the first order in $\sqrt{\delta}$, the solution of Eq. (11) is

$$\zeta^0 = A(T) + Br - \int_0^r dt\int_0^t d\xi\left(\frac{\partial_\theta\tilde{w}_a(\xi)}{\xi}\right)^0. \qquad (13)$$

The constant B and function $A(T)$ are determined from the matching conditions. The functions $M_\mu(T)$ can be found by solving Eqs. (11)–(13) and keeping only terms up to the order of $\sqrt{\delta}$. The result is $M_i^0 = 0$, $M_0^1 = \Delta_2 - N_1^0/2$, and

$$M_{2i}^1 = 2\Delta_2 - \frac{1}{2}\left[4\Omega^2\sum_{k=1}^{i}(2k-1)N_{2(i-k)+1}^0 + N_{2i-1}^0 + N_{2i+1}^0\right],\ i = 1,2\ldots, \qquad (14)$$

$$M_{2i+1}^1 = 2(2i+1)B\Omega^2 - 2\Omega\left[\sum_{k=0}^{i}N_{2k+1}^0 - (i+1)N_{2i+1}^0\right],\ i = 0,1\ldots, \qquad (15)$$

where $\Delta_2 = \Omega\sqrt{\delta}A'(T) + \Omega^2 A(T) + \Omega B - f(T)$. Observe that Eqs. (14) and (15) confirm our initial assumption (10). Next, we derive an equation for the δ correction to the front perturbation. Keeping δ- and $\delta^{3/2}$-order terms in Eq. (11) yields

$$\partial_r^2\zeta^1 = -A''(T) - \Omega\sqrt{\delta}A'(T) - \Omega\partial_r\zeta^0 - \left(\frac{\partial_\theta\tilde{w}}{r}\right)^1 + f(T). \qquad (16)$$

Following the standard procedure of the multiple-scale analysis, we eliminate the secular terms in the last equation. This condition gives the following differential equation for $A(T)$:

$$A''(T) + \sqrt{\delta}\Omega A'(T) + \Omega\left(B + C_t\right) + \left(\frac{\partial_\theta \tilde{w}}{r}\right)^1\Bigg|_{r\to\infty} = f(T), \qquad (17)$$

where

$$\left(\frac{\partial_\theta \tilde{w}}{r}\right)^1 = \frac{1}{2}\Bigg[N_1^1 J_0(r) + N_2^1 J_1(r) + \sum_{\mu=2}^{\infty} J_\mu(r)\left(N_{\mu-1}^1 + N_{\mu+1}^1\right)\Bigg], \qquad (18)$$

and $C_t = -\sum_{i=0}^{\infty} N_{2i+1}^0$. The functions $N_\mu(T)$ can be found by solving Eqs. (5) and (6). After some straightforward algebra, in the limit of $\mu >> 1$, we obtain $N_\mu^1 \simeq M_\mu^1$, and Eq. (18) becomes

$$\left(\frac{\partial_\theta \tilde{w}}{r}\right)^1\Bigg|_{r\to\infty} = \Delta_2 - C_1\Omega^2 + \Omega C_t + \left(B + C_t\right)\Omega^2 r, \qquad (19)$$

where $C_1 = -\sum_{i=0}^{\infty}(2i+1)N_{2i+1}^0$. Eliminating the secular terms in Eq. (16) with the help of Eq. (19) gives $B = -C_t$, and

$$A'' + 2\sqrt{\delta}\Omega A' + \Omega^2 A = 2f(T) + \Omega^2 C_1. \qquad (20)$$

Substituting Eq. (20) into Eq. (13) and using the fact that the coefficients $N_{i>3}^0$ are numerically small for an arbitrary Mach number M_1 yields

$$\frac{\eta_a\left(kc_s t >> 1\right)}{\eta_0} = \Sigma_3 e^{kV_a t}\int_{\infty}^{-kV_a t/\sinh\theta_s} e^{\eta\sinh\theta_s} J_1(\eta)\,d\eta + \left[\frac{c_s\Sigma_2}{\sqrt{V_a V_{\rm bl}}}\sin\omega t + \left(1 - \Sigma_1 + \Sigma_4\right)\cos\omega t\right]e^{-2kV_a t}, \qquad (21)$$

where $\omega = k\sqrt{V_a V_{\rm bl}}$ and

$$\Sigma_0 = \frac{16(M_1^2-1)M_1^2}{\left(2\gamma M_1^2 - \gamma + 1\right)\left(3M_1^2 + 1\right)},$$

$$\Sigma_1 = 2\Sigma_0\frac{M_1^4(5\gamma-1) + 2M_1^2(\gamma+3) - 3\gamma - 1}{M_1^4(17\gamma-7) + 2M_1^2(\gamma+9) - 3\gamma + 5},$$

$$\Sigma_2 = \frac{1}{3}\left(\Sigma_0 + \Sigma_1\right),$$

$$\Sigma_3 = \frac{\Sigma_0}{L_1}\left(\frac{4}{\gamma+1} - L_2 - L_3\right)\frac{\sinh^2\theta_s}{\Omega},$$

$$\Sigma_4 = \Sigma_3\left(1 - \tanh\theta_s\right).$$

Equation (21) shows that the ablation-front perturbations oscillate in time with the frequency ω proportional to the ablation velocity V_a. In addition, the amplitude of oscillations is damped by the mass ablation [term $e^{-2kV_a t}$ in Eq. (21)]. The period of oscillations is much smaller, however, than the damping rate $kV_a/\omega = \sqrt{V_a/V_{\rm bl}} = \sqrt{\delta} << 1$. In the limit of zero ablation velocity, $\sin\omega t \simeq k\sqrt{V_a V_{\rm bl}}\,t$, and Eq. (21) leads to a classical asymptotic linear growth $\eta\left(kc_s t >> 1\right) \simeq \eta_0\left(1 - \Sigma_1 + kc_s\Sigma_2 t\right)$.

The oscillatory behavior of the perturbations can be explained on the basis of the following simple model. Let us consider a slab of a uniform-density fluid with the perturbed right interface. If the applied pressure at the left and right sides of the slab is P_L and P_R, then the effective acceleration experienced by the slab is $g_{\rm eff} = -\left(P_R - P_L\right)/M$, where $M = \rho L$ is the mass of the slab and L is its length. In the case where the effective acceleration is pointing in the direction from a perturbed interface toward the slab, such a configuration is hydrodynamically stable, and any surface perturbations oscillate in time (gravity wave). For a target driven by a laser irradiation, the dynamic pressure in the blowoff region $P_R = \rho_3 V_{\rm bl}^2 = \rho_2 V_a V_{\rm bl}$ is greater than the dynamic pressure in the shock-compressed region $P_L = \rho_2 V_a^2 = P_R\delta < P_R$, and the effective acceleration is pointing in the direction of the density gradient (from the perturbed ablation surface toward the shock compressed region). From the equation describing the temporal evolution of a gravity wave $\ddot{\eta} = kg_{\rm eff}\eta$, it follows

that the frequency of oscillations is $\omega = \sqrt{-kg_{\rm eff}} \simeq \sqrt{kV_aV_{\rm bl}/L}$, and we recover the result of Eq. (21) with $L = 1/k$. The simple model described above shows that the dynamic overpressure is the main stabilizing mechanism of the ablation-surface perturbations during the shock-transit time. The estimate of the oscillation frequency can be also obtained by using the result of the self-consistent theory of the ablative RT instability.[6–8] For the large Froude number case (small acceleration), the perturbation growth rate is $\gamma \simeq \sqrt{kg - k^2V_aV_{\rm bl}} - 2kV_a$. Taking the limit of $g \to 0$ in the last expression gives the oscillation frequency $\omega = i\gamma = k\sqrt{V_aV_{\rm bl}}$, in agreement with Eq. (21).

For a quantitative comparison of the model [Eq. (21)] with the result of numerical simulations, one needs to estimate the value of blowoff velocity $V_{\rm bl}$. Simulations and the self-consistent analysis of ablation fronts[6–8] show that the velocity of ablated plasma is not uniform, and it increases in the direction toward the blowoff plasma. As shown in Refs. 7, 8, and 10, however, the appropriate value of the blowoff velocity to be substituted into the sharp-boundary model is $V_{\rm bl} \equiv V_a/\delta = V_a/\left[\mu(\nu)(kL_0)^{1/\nu}\right]$, where ν is the power index for the thermal conduction, L_0 is the characteristic thickness of ablation front (proportional to the minimum density-gradient scale length),[7] $\mu = (2/\nu)^{1/\nu}/\Gamma(1+1/\nu) + 0.12/\nu^2$, and $\Gamma(x)$ is the gamma function. The effective power index ν and the thickness of the ablation front L_0 can be determined by fitting the hydrodynamic profiles obtained using the 1-D hydrodynamic code with the solution of the isobaric model.[12] For plastic (CH) targets directly driven by a flat-top laser pulse with an intensity of 50 to 200 TW/cm^2, $L_0 \simeq 0.1\,\mu$m, $\nu \simeq 1$, and the oscillation period is

$$T_{\rm CH} \simeq 2.8/\left[V_a(\mu\text{m/ns})\sqrt{k(\mu\text{m}^{-1})}\right] \text{ ns}.$$

Cryogenic DT targets have a much smaller density-gradient scale length $L_0 \simeq 0.01\,\mu$m, $\nu \simeq 2$, and

$$T_{\rm DT} \simeq 2/\left[V_a(\mu\text{m/ns})k^{3/4}(\mu\text{m}^{-1})\right] \text{ ns}.$$

For the cryogenic NIF target designs, $V_a \simeq 2\,\mu$m/ns during the shock-transit time, and $T_{\rm DT} = 2.5$ ns for 20-μm perturbation wavelength. In this case the ablation-front perturbations will experience several oscillations (the breakout time for such targets is around 5 ns). Figure 77.32 shows the front-perturbation evolution of the 200-μm-thick DT foil driven by a square pulse with an intensity of 100 TW/cm^2. The initial amplitude of perturbation is 0.1 μm, and its wavelength is 20 μm. The dots represent the result of 2-D hydrocode *ORCHID*,[13] and the solid line shows the prediction of the sharp-boundary model. Observe that the analytic formula (21) reproduces not only the period of oscillation but also its amplitude.

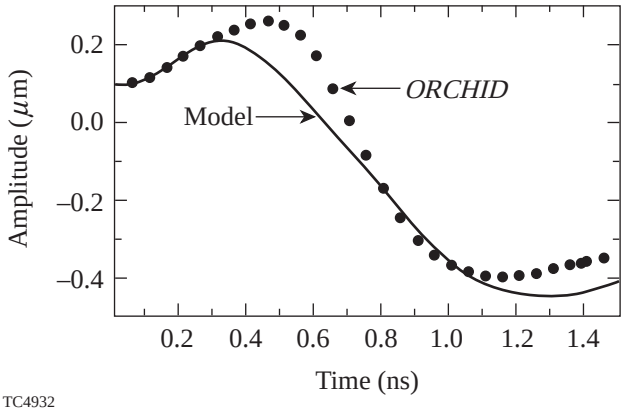

Figure 77.32
Time evolution of the ablation-front perturbation calculated using analytic formula (22) (solid line) compared with the numerical results (dots) of the 2-D hydrocode *ORCHID*.

In summary, the analytic theory of the ablative Richtmyer–Meshkov instability was developed. It was shown that the main stabilizing mechanism of the ablation-front perturbations is the dynamic overpressure of the blowoff plasma with respect to a target material.

ACKNOWLEDGMENT

The author thanks Professors R. Betti and J. Sanz and Dr. C. Cherfils for helpful discussions. This work was supported by the U.S. Department of Energy Office of Inertial Confinement Fusion under Cooperative Agreement No. DE-FC03-92SF19460, the University of Rochester, and the New York State Energy Research and Development Authority. The support of DOE does not constitute an endorsement by DOE of the views expressed in this article.

REFERENCES

1. R. D. Richtmyer, Commun. Pure. Appl. Math. **XIII**, 297 (1960).

2. S. E. Bodner, D. G. Colombant, J. H. Gardner, R. H. Lehmberg, S. P. Obenschain, L. Phillips, A. J. Schmitt, J. D. Sethian, R. L. McCrory, W. Seka, C. P. Verdon, J. P. Knauer, B. B. Afeyan, and H. T. Powell, Phys. Plasmas **5**, 1901 (1998).

3. R. Ishizaki and K. Nishihara, Phys. Rev. Lett. **78**, 1920 (1997).

4. R. J. Taylor *et al*., Phys. Rev. Lett. **79**, 1861 (1997).

5. A. L. Velikovich *et al*., Phys. Plasmas **5**, 1491 (1998).

6. J. Sanz, Phys. Rev. Lett. **73**, 2700 (1994).

7. V. N. Goncharov, R. Betti, R. L. McCrory, P. Sorotokin, and C. P. Verdon, Phys. Plasmas **3**, 1402 (1996).

8. V. N. Goncharov, "Self-Consistent Stability Analysis of Ablation Fronts in Inertial Confinement Fusion," Ph.D thesis, University of Rochester, 1998.

9. P. M. Zaidel, J. Appl. Math. Mech. **24**, 316 (1960).

10. A. R. Piriz, J. Sanz, and L. F. Ibanez, Phys. Plasmas **4**, 1117 (1997).

11. S. E. Bodner, Phys. Rev. Lett. **33**, 761 (1974).

12. R. Betti, V. N. Goncharov, R. L. McCrory, and C. P. Verdon, Phys. Plasmas **5**, 1446 (1998).

13. R. L. McCrory and C. P. Verdon, in *Computer Applications in Plasma Science and Engineering*, edited by A. T. Drobot (Springer-Verlag, New York, 1991).